

Supplementary Materials: Catalytic mechanism comparison between 1,2-dichloroethane-acetylene exchange reaction and acetylene hydrochlorination reaction for vinyl chloride production: DFT calculations and experiments

Hao Xu *, Baochang Man and Guohua Luo *

Beijing Key Laboratory of Green Chemical Reaction Engineering and Technology,
Department of Chemical Engineering, Tsinghua University, Beijing 100084, China; mbcthu@163.com

* Correspondence: xh14@mails.tsinghua.edu.cn (H.X.); luoguoh@tsinghua.edu.cn (G.L.);
Tel.: +1-587-887-2735 (H.X.); Tel.: +86-10-62788994 (G.L.)

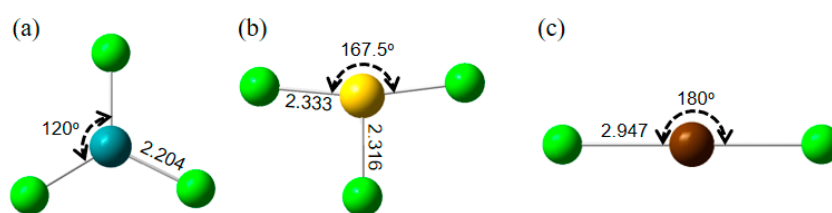


Figure S1. Structures of metal chlorides, (a) RuCl₃, (b) AuCl₃, (c) BaCl₂. Unit of length and angle are Å and degree respectively.

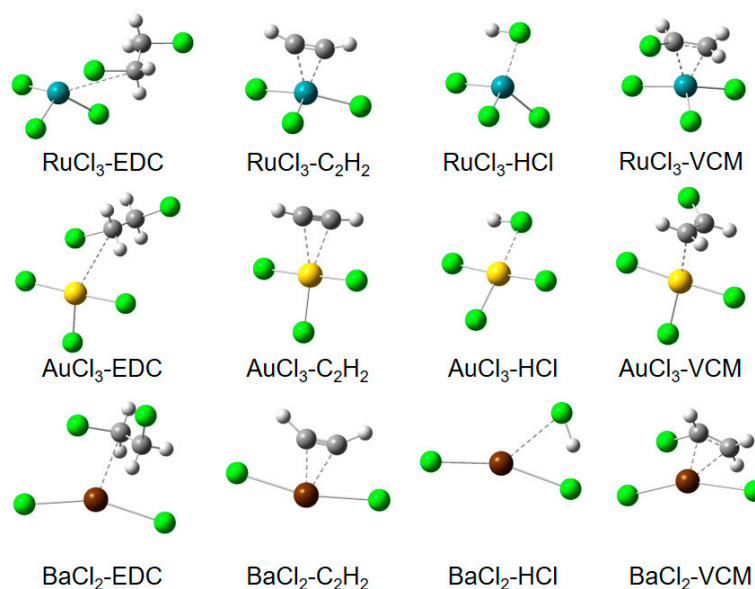


Figure S2. Optimized structure of adsorbed species on metal chloride surfaces.

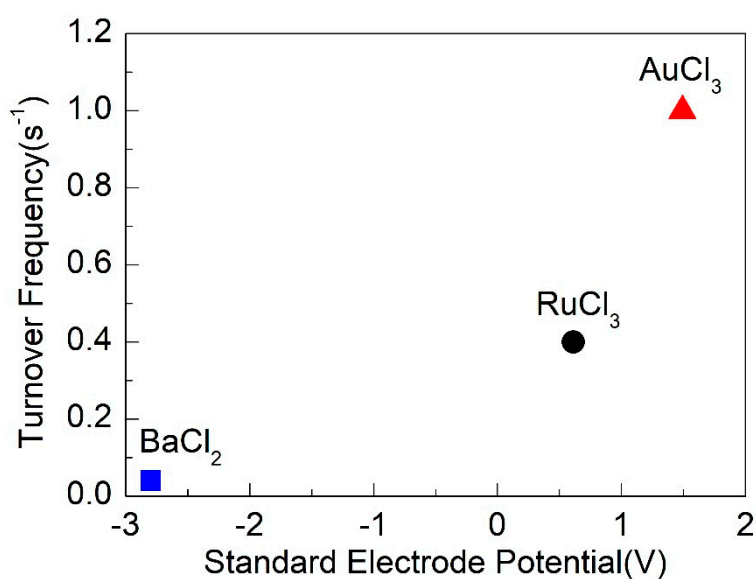


Figure S3. Catalytic turnover frequency of three metal chlorides for acetylene hydrochlorination reaction.

Table S1. Main structure parameters of important species after adsorption. M stands for the metal atoms in metal chlorides. Bond length unit: Å, angle unit: degree. Value in parentheses are corresponding values in free molecules.

	Catalyst	RuCl ₃	AuCl ₃	BaCl ₂
	Bond M-C	2.113	2.416	2.317
C ₂ H ₂	Bond C≡C(1.204)	1.253	1.223	1.260
	Angle C≡C-H(180)	160.2	173.5	146.7
HCl	Bond M-Cl	2.634	2.588	3.271
	Bond H-Cl(1.288)	1.301	1.301	1.434
VCM	Bond M-C	2.154	2.324	2.087
	Bond C=C(1.326)	1.407	1.378	1.423
DCE	Bond M-C	3.691	3.665	2.962
	Bond C-C(1.518)	1.521	1.525	1.535

Table S2. Absolute energies in Hartrees of calculated species in DCE decomposition reaction pathway for DCE-acetylene exchange reaction.

M=	RuCl ₃	AuCl ₃	BaCl ₂
M	-1474.48309730	-1516.01939101	-945.70684237
DCE	-999.01899897	-999.01899897	-999.01899897
HCl	-460.79569406	-460.79569406	-460.79569406
C ₂ H ₂	-77.32564618	-77.32564618	-77.32564618
C ₂ H ₃ Cl	-538.18539427	-538.18539427	-538.18539427

Ads	-2473.51070364	-2515.06176981	-1944.77268772
TS1	-2473.55043638	-2515.05799345	-1944.82105039
IM1	-1935.30298898	-1976.83809341	-1406.56862043
IM2	-2012.71242646	-2054.21686615	-1483.97324675
TS2	-2012.65798338	-2054.16905957	-1483.91238328
Des	-2012.71605016	-2054.24683263	-1483.94800797

Table S3. Absolute energies in Hartrees of calculated species in acetylene-DCE complex reaction pathway for DCE-acetylene exchange reaction.

M=	RuCl ₃	AuCl ₃	BaCl ₂
M	-1474.48309730	-1516.01939101	-945.70684237
DCE	-999.01899897	-999.01899897	-999.01899897
HCl	-460.79569406	-460.79569406	-460.79569406
C ₂ H ₂	-77.32564618	-77.32564618	-77.32564618
C ₂ H ₃ Cl	-538.18539427	-538.18539427	-538.18539427
Ads	-1551.86564162	-1593.38542602	-1023.09417172
IM1	-2550.88096418	-2592.40268405	-2022.11786347
TS1	-2550.84079343	-2592.36204573	-2022.09907915
IM2	-2012.71989372	-2054.24590692	-1483.97138318
TS2	-2012.66668368	-2054.20075059	-1483.90819759
Des	-2012.71605016	-2054.24683263	-1483.94800797

Table S4. Absolute energies in Hartrees of calculated species for acetylene hydrochlorination reaction.

M=	RuCl ₃	AuCl ₃	BaCl ₂
M	-1474.48309730	-1516.01939101	-945.70684237
HCl	-460.79569406	-460.79569406	-460.79569406
C ₂ H ₂	-77.32564618	-77.32564618	-77.32564618
C ₂ H ₃ Cl	-538.18539427	-538.18539427	-538.18539427
Ads	-1551.86564162	-1593.38542602	-1023.09417172
IM1	-1551.91123129	-1593.43123138	-1483.97138318
TS1	-1551.84867916	-1593.38258504	-1483.85316941
IM2	-1551.86756777	-1593.43017751	/
TS2	-2012.65654542	-2054.20465095	/
Des	-2012.71605016	-2054.24683263	-1483.94800797

Reaction evaluation process of DCE-acetylene exchange reaction

Figure S4 is the diagram for the reaction evaluation equipment. A typical evaluation procedure is given as follows: First, 2.0000 g catalyst was put into a U-shaped silica tube reactor with quartz wool on both sides (inner diameter 6 mm) and the reactor was placed in the reaction furnace. Then N_2 (99.999%, Beijing Beiwen Gas Works) controlled by rotor flowmeter was fed continuously to further desiccate the catalyst for 30 min with a volume flow rate of 20 mL min^{-1} . Next, DCE (99.9%, aladdin) was fed with a volume flow rate of $0.022 \text{ mL min}^{-1}$ by a high pressure liquid sampling pump (FL2200, Zhejiang Fuli Co., Ltd.) and passed through a preheating furnace to get fully gasified. Both furnaces were set to the reaction temperature in advance. After activating the catalyst by DCE for 30 min, acetylene (99.99%, Beijing Fuxingrui Industrial Gas Co., Ltd) controlled by a mass flowmeter (D07-19B, Beijing Qixinghuachuang Co., Ltd.) was fed with a volume flow rate of 6 mL min^{-1} (corrsponding to 90 h^{-1} gas hourly space velocity). A volume ratio of gaseous DCE: $C_2H_2=1.1:1$ was maintained during the evaluation. The outlet gas was first passed through a condenser to condense unreacted DCE and then dessicated in a dryer filled with anhydrous calcium chloride. Next, gas chromatography (GC7890T, Zhejiang Fuli Co., Ltd., thermal conductivity detector) was used to determine the acetylene conversion. An adsorption bottle was connected at the end of gas line to trap the effluent gas. Samples were collected every 15 minutes and the conversion was determined by the ratio of peak areas, which were calibrated by standard gas mixture (Beijing Beiwen Gas Works).

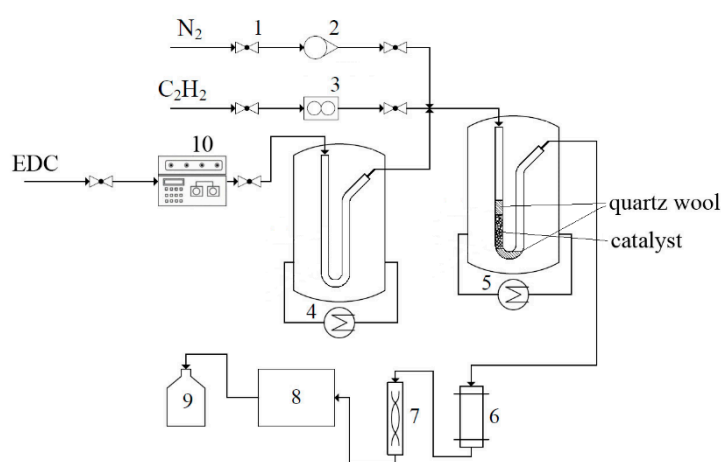


Figure S4. Diagram of the experimental equipment (1) Controlling valve; (2) Rotor flowmeter; (3) Mass flowmeter; (4) Preheating furnace; (5) Reaction furnace; (6) Condenser; (7) Dryer; (8) Gas chromatography; (9) Exhausted gas absorption bottle; (10) High pressure liquid sampling pump.

Kinetic study

This reaction is a typical gas-solid phase reaction and complies with a seven-step reaction mechanism including external diffusion, internal diffusion and surface reaction. Kinetic study requires excluding the influence of external and internal diffusion to get the intrinsic kinetic parameters.

A plug flow reactor (PFR) model was adopted in the following discussion. To justify the validity of the model, the length-diameter ratio L/D of our reactor was calculated to be 30 and the Reynolds number Re was calculated to be 3383. These values were sufficiently large to ensure the flow properties of a PFR model.

In order to evaluate the influence of external diffusion of the reactor, a typical $BaCl_2$ catalyst was operated under the same space velocity with various catalyst loadings. To keep the space velocity identical, the volume flux of the feed gas was kept proportional to the catalyst loading. Specifically, different catalyst loadings of 1.0000, 2.0000 and 3.0000 g were selected and the corresponding volume fluxes of acetylene were 3.00, 6.00 and 9.00 standard-state cubic centimeter per minute (scm)

respectively, keeping a GHSV of 90 h⁻¹. Due to low conversion and small heating effect of the reaction, the temperature difference caused by various gas volume fluxes was negligible (less than 0.3 °C in observation). Experimental results were shown in Figure S5.

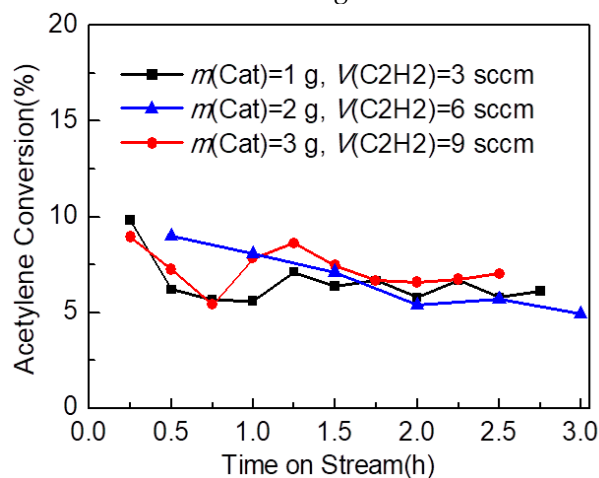


Figure S5. Reaction evaluation of BaCl₂ catalysts with different catalyst loadings at constant GHSV. Reaction conditions: $T=220$ °C, GHSV=90 h⁻¹, $V(\text{C}_2\text{H}_2)/V(\text{DCE})=1:1.1$.

It can be seen that the acetylene conversion remained similar with different catalyst loadings at same GHSV, indicating external diffusion resistance is negligible for this reaction.

Next, in order to evaluate the influence of internal diffusion, a series of typical BaCl₂ catalysts with different support particle sizes (specifically, 30-100 mesh, 60-80 mesh and 80-100 mesh) were prepared and operated under same reaction condition. Results were shown in Figure S6.

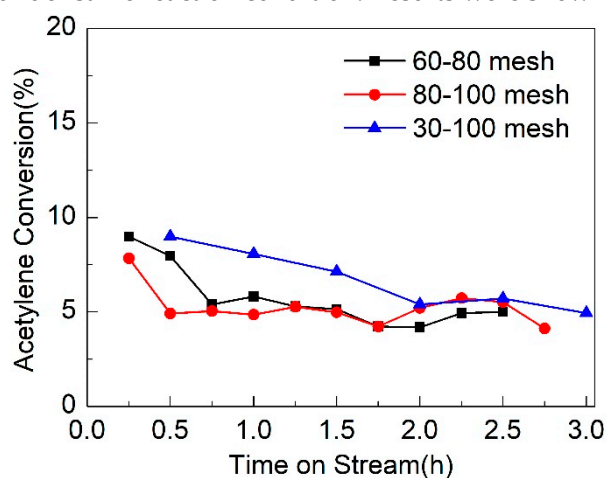


Figure S6. Reaction evaluation of BaCl₂ catalysts with different average sizes of support. Reaction conditions: $T=220$ °C, GHSV=90 h⁻¹, $V(\text{C}_2\text{H}_2)/V(\text{DCE})=1:1.1$.

As shown in Figure S6, the activities of catalysts were similar with different sizes of support. Therefore, internal diffusion demonstrates no significant influence on this reaction.

The theoretical reaction order to each reactant can be derived from the proposed mechanism with acetylene-DCE complex pathway by applying equilibrium hypothesis. Since the rate determining step is behind the adsorption of C₂H₂ and DCE, the reaction is theoretically first order to both C₂H₂ and DCE. Experimental were also carried out to determine the reaction order to each reactant with various volume fluxes of C₂H₂ and DCE. Considering that C₂H₂ can lead to fast deactivation of catalysts due to self polymerization, the amount of DCE was set to be excessive in subsequent experiments. Results can be seen in Figure S7. Since the catalysts underwent fast deactivation, only the average conversion data of the first hour were used to determine the reaction

rate. The reaction order of each reactant was then derived by multiple regression of the reaction rate equation:

$$r = k[\text{C}_2\text{H}_2]^a[\text{DCE}]^b$$

Where r is the reaction rate, k is the rate constant, a and b are reaction orders to C_2H_2 and DCE respectively.

The regression result gave $a=1.30$ and $b=0.98$, which were both close to 1, indicating the assumption that the reaction is first order to both C_2H_2 and DCE is reasonable. Namely, the rate equation can be written as:

$$r = k[\text{C}_2\text{H}_2][\text{DCE}]$$

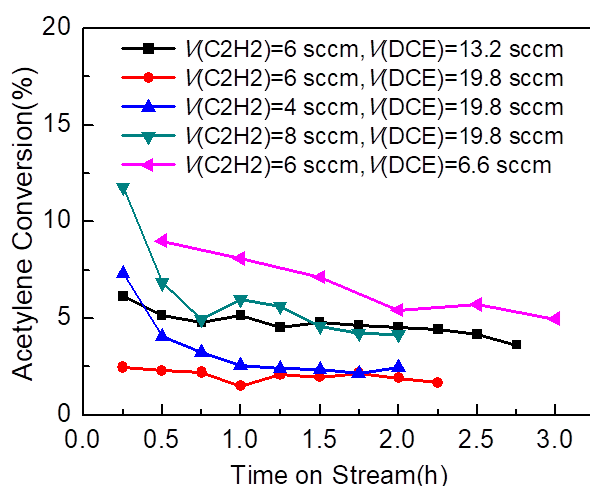


Figure S7. Reaction evaluation of BaCl_2 catalysts with different C_2H_2 and DCE gaseous volume flux. Reaction conditions: $T=220\text{ }^\circ\text{C}$.

Finally, after the kinetic study, all catalysts were evaluated at different temperature to get the activation energy. The corresponding rate constant k was calculated according to the kinetic model and corresponding data were shown in Figure 4.

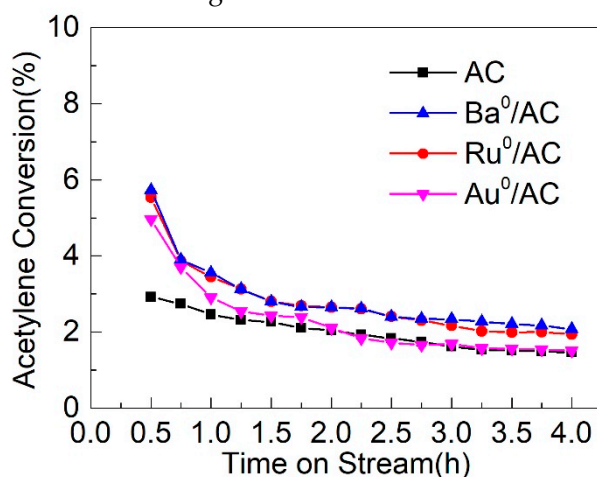


Figure S8. Reaction evaluation of activated carbon support and reduced zero-valance metal catalysts. The reduction process was realized by treating prepared catalysts with sodium borohydride solution with excessive NaBH_4 reduction capability. Reaction conditions: $T=260\text{ }^\circ\text{C}$, $\text{GHSV}=90\text{ h}^{-1}$, $V(\text{C}_2\text{H}_2)/V(\text{DCE})=1:1.1$. The acetylene conversion was significantly lower than metal catalysts with high valences of metals.



© 2020 by the authors. Submitted for possible open access publication under the terms and conditions of the Creative Commons Attribution (CC BY) license (<http://creativecommons.org/licenses/by/4.0/>).